


Effects of process parameters on cutting forces, material removal rate, and specific energy in trochoidal milling

Proc IMechE Part C:
J Mechanical Engineering Science
1–13
© IMechE 2023
Article reuse guidelines:
sagepub.com/journals-permissions
DOI: 10.1177/09544062231196991
journals.sagepub.com/home/pic


Mohamed Wagih^{1,2} , Mohsen A Hassan^{1,3}, Hassan El-Hofy⁴,
Jiwang Yan⁵  and Ibrahim Maher^{1,6}

Abstract

Trochoidal milling has been developed to enhance tool life during slot machining. It is characterized by reduced cutting forces, cutting temperature, and tool wear as compared to conventional milling processes. It is effective in machining difficult-to-cut materials, high-speed machining, and groove corners. However, this process has not been deeply investigated enough to discover its advantages and optimize its parameters. A full factorial design of 144 experiments has been applied in this paper to investigate extensively the effects of axial depth of cut, feed rate, and trochoidal step on material removal rate, cutting forces, and specific energy in trochoidal milling. Trochoidal step and axial depth of cut almost have the same contributions on cutting forces by 32% and 31% respectively, followed by feed rate by 25%. Feed rate, trochoidal step, and axial depth of cut influence the material removal rate by 37%, 30%, and by 19% respectively. The contributions of feed rate, trochoidal step, and axial depth of cut on relative specific energy are 57%, 24%, and 8% respectively. The increase of axial depth of cut increases the maximum resultant force till a threshold value, then it stabilizes. This behavior occurred due to the increase of the maximum engagement angle to a certain limit, then it does not increase any more. Both feed rate and trochoidal step linearly affect maximum resultant force and material removal rate, while the relationships are non-linear for specific energy. It is recommended to machine slots in full depth with the highest possible trochoidal step and feed rate, considering the increase of tool wear and surface roughness. It is preferred to use a cutting tool of a large helix angle and small diameter to reduce the threshold axial depth of cut. Overall, this study is significant in characterizing, designing, and optimizing of trochoidal milling through experimental work.

Keywords

Trochoidal milling, cutting forces, material removal rate, specific energy

Date received: 22 May 2023; accepted: 4 August 2023

Introduction

Trochoidal milling, Figure 1, is a milling process that has been developed to enhance the cutting tool life by introducing a cooling path after each cutting path. In this process, a rotating cutting tool with a speed n , moves typically in a predetermined closed path with a feed rate f_r . After each revolution, the tool translates linearly a distance defined as trochoidal step, s . Cutting is performed in the linear part and half of the circular part of the tool path, then the cutting tool is cooled down in the other half, improving the tool life and consequently the process cost-effectiveness. The tool path is typically circular, but there are other developed types, such as true trochoidal, elliptical, etc., to improve the process efficiency.^{1–3} Since the

¹Department of Industrial and Manufacturing Engineering, Egypt-Japan University of Science and Technology, Alexandria, Egypt

²Design and Production Department, Faculty of Engineering, Ain Shams University, Cairo, Egypt

³Mechanical Engineering Department, Faculty of Engineering, Assiut University, Assiut, Egypt

⁴Production Engineering Department, Faculty of Engineering, Alexandria University, Alexandria, Egypt

⁵Department of Mechanical Engineering, Faculty of Science and Technology, Keio University, Yokohama, Japan

⁶Department of Mechanical Engineering, Faculty of Engineering, Kafrelsheikh University, Kafrelsheikh, Egypt

Corresponding author:

Mohamed Wagih, Faculty of Engineering, Ain Shams University, 1 Elsarayat St., Abbaseya, Cairo 11517, Egypt.

Email: mwagih@eng.asu.edu.eg

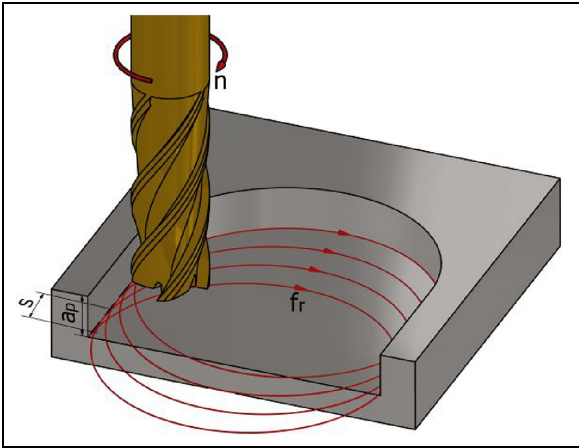


Figure 1. Schematic drawing of circular type trochoidal milling process.

tool diameter is less than the slot width, the engagement angle between tool and workpiece is lower as compared to that of conventional milling. Therefore, cutting forces, cutting temperature, and tool wear are lower.^{1,4,5} Trochoidal milling is efficient in the machining of difficult-to-cut materials such as Ti-6Al-4V,⁵⁻⁸ duplex stainless steel,⁹ Inconel superalloys,^{10,11} etc., in high-speed machining^{12,13} and machining of corners.^{14,15} Uddin et al. proved experimentally that trochoidal milling is suitable for deep and narrow grooves.¹⁶ On the other hand, the process suffers from a lower material removal rate and surface finish as compared to conventional milling under the same cutting conditions due to the process kinematics.^{1,17}

Several efforts have been exerted to improve the material removal rate in trochoidal milling through optimization of process parameters or development of new techniques or paths. The increase of material removal rate, by increasing process parameters, is constrained by machine tool and cutting tool capabilities, product accuracy, and surface finish requirements. This can be related to the accompanied increase of cutting forces,^{6,18} tool temperature,¹⁹ tool wear,^{9,20} surface roughness,^{18,19,21} etc. Hence, in order to improve material removal, these factors should be considered. Szalóki et al. studied experimentally the effects of axial depth of cut, trochoidal step, and feed per tooth on material removal rate during true trochoidal milling of 40CrMnMo7 alloy.¹⁸ They conducted only six experiments out of 27 available ones, where only two levels of each variable have been investigated. They concluded that trochoidal step has the most significant effect on material removal rate, followed by feed per tooth, and then axial depth of cut. They built their conclusions and statistical models on only two points on the curve. M. Otkur and I. Lazoglu concluded that using double trochoidal milling, as an alternative to conventional trochoidal milling, can improve the material removal rate by 50%, but the cutting forces raised by the same ratio and the cooling path has been

eliminated.²² Salehi et al. improved the material removal rate by 20% on using a developed epicycloidal tool path at the expense of a 10% increase in the forces.² However, it has been proved that dynamic trochoidal milling and variable feed trochoidal milling are better than the static one,^{23,24} but high-dynamic machine tools are required. Adaptive trochoidal milling with a variable step or a variable trochoidal radius showed its capability to stabilize the cutting forces along the tool path, consequently, the material rate has been improved.^{15,25}

Cutting forces are principal factors that determine cutting power, machine tool loads, cutting temperature, tool life, etc., to select the machine tool, cutting tool, and process parameters.²⁶ Studies regarded to cutting forces are either analytical or experimental. The analytical studies focus on the modeling of cutting forces using the determination of chip thickness and coefficients of cutting forces.^{27,28} The experimental studies give a more comprehensive investigation of the process, as it includes other parameters which will complicate the analytical models if they are considered, such as system stability, built-up edge, etc.²⁹ In addition to material removal rate, Szalóki et al. studied the effects of axial depth of cut, trochoidal step, and feed per tooth on cutting forces.¹⁸ They found that trochoidal step has the most significant effect on increasing the cutting forces, followed by the axial depth of cut, and then the feed per tooth. Oh et al. studied the effects of feed per tooth and cutting speed during trochoidal milling of Ti-6Al-4V alloy.⁶ The results proved that feed per tooth has a significant effect on cutting forces while cutting speed has not. They considered three levels of feed per tooth and two for cutting speed. Šajgalik et al. examined the effects of both trochoidal step and engagement angle on the resultant cutting force for hardened steel trochoidal milling.³⁰ They selected three levels of each. They found that the engagement angle is more significant than the trochoidal step in increasing the cutting force. In their study, Pleta et al. concluded, during trochoidal milling of Inconel 738, that axial depth of cut has the greatest influence on resultant forces followed by feed rate, and then the cutting speed.³¹ They used only two levels of each. Other researchers proved that tool path considerably affects cutting forces.^{1,2,32}

Specific energy, U , is being employed to evaluate the process efficiency.^{6,19} It can be defined as the consumed energy, E , to remove a unit volume of work material, MRV , or the ratio between cutting power, P , to material removal rate, MRR , equation (1).^{6,33} The cutting power is the product of tangential force, F_t , and cutting speed, v . In the studies by Santhakumar and Iqbal,¹⁹ and by Oh et al.⁶ the effects of cutting parameters on specific energy have been investigated. They observed that the increase of feed per tooth or cutting speed decreases specific energy slightly because each of them affects both cutting forces and material removal rate with almost the same value

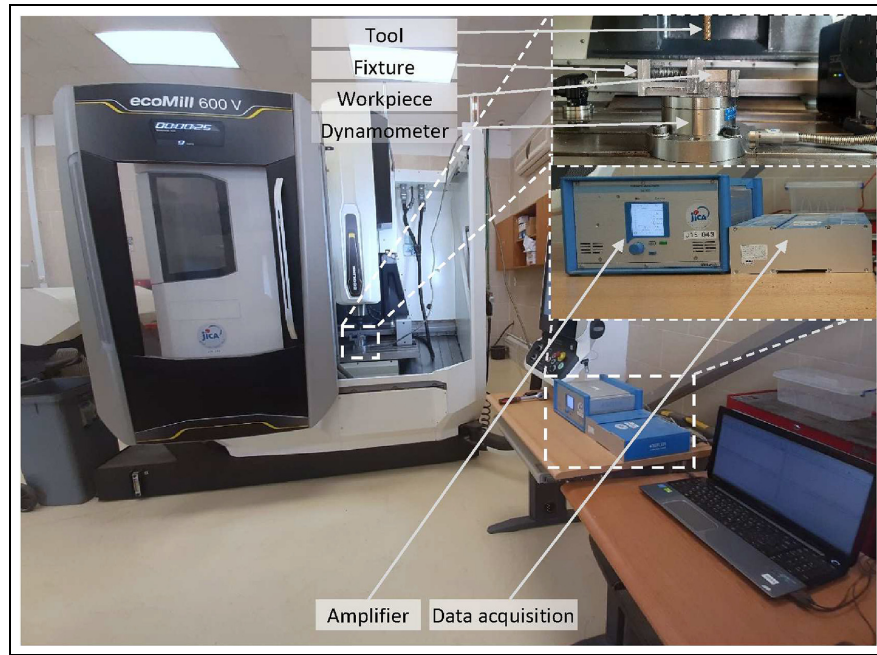


Figure 2. Experimental setup and measuring system used in experiments.

Table 1. Chemical composition of P20 steel alloy.

Element	C	Cr	Fe	Mn	Mo	P	S	Si	Other
Content (wt%)	0.374	1.8	95.6	1.44	0.259	0.0064	< 0.0005	0.299	< 0.07

$$U = \frac{E}{MRV} = \frac{P}{MRR} = \frac{F_t v}{MRR} \quad (1)$$

The discussed literature showed that there are limited research papers that studied the effects of cutting parameters on material removal rate, cutting forces, and specific energy simultaneously. Even these papers include only two levels for each parameter. This paper aims to investigate extensively the effects of axial depth of cut, feed rate, and trochoidal step, on cutting force, material removal rate, and relative specific energy during trochoidal milling process. This study is significant in characterizing, designing, and optimizing of trochoidal milling.

Materials and methods

In this section, the equipment, materials, and measuring devices will be presented, in addition to the applied design of experiments.

Equipment and measurements

The experiments have been conducted on DMG Mori ecoMill 600V CNC milling machine tool of 12,000 rpm maximum speed, 20,000 mm/min maximum feed rate, and 1 μ m table resolution in all

directions. It is equipped with Siemens Sinumerik 840D. Figure 2 shows the experimental setup and the measuring system. The workpiece material used was P20 alloy steel in an unhardened state, where its chemical composition is shown in Table 1. This alloy is used in molds and dies manufacturing and other tooling applications due to its mechanical properties and good machinability. The workpiece was 60 mm width, 20 mm length, and 15 mm thickness. In order to reduce the setting time and number of specimens, several experiments have been executed on each workpiece. The circular type trochoidal milling has been applied to machine a slot of 20 mm length and 20 mm width using the conditions shown in Table 2. In the present work, the process parameters have been selected based on recommendations of pilot experiments as given by ASM handbook Machining, volume 16. The pilot experiments will ensure avoiding tool failure that may occur beyond the selected machining conditions.³⁴ All the experiments have been performed under dry conditions. Before the implementation of the experiments, face milling of the upper surface was applied to determine the reference plane for the axial depth of cut. A square endmill of model P-SE1004 SI from PAN TIGER has been used in the experiments. The cutting tool was TiSiN-coated carbide of 10 mm diameter, four teeth, and 35° helix angle.

Table 2. Process parameters in trochoidal milling experiments.

Parameter	Examined levels
Axial depth of cut, a_p (mm)	2, 4, 6, 8
Tool center feed rate, f_r (mm/min)	400, 600, 800, 1000
Tool center feed per tooth, f_z (mm/tooth)	0.05, 0.075, 0.1, 0.125
Tool edge feed per tooth, f_{ze} (mm/tooth)	0.1, 0.15, 0.2, 0.25
Trochoidal step, s (mm)	0.5, 1, 1.5
Rotational speed, n (rpm)	2000

Table 3. Sample of the 144 implemented experiments.

Run order	a_p (mm)	s (mm)	f_r (mm/min)
1	4	1.5	1000
2	6	1.5	600
3	6	1.5	400
4	4	1	600
5	2	1.5	600
6	4	1.5	600
7	2	0.5	600

The used forces measuring system consists of Kistler 4-component dynamometer type 9272, charge amplifier type 5070A, and data acquisition type 5679A. The dynamometer is a piezoelectric type of measuring ranges -5.5 kN in x and y directions and -5.20 kN in z direction. The data acquisition can read up to 10^6 total sampling rates for the four channels equipped in the amplifier. The measured forces signals are converted into charges, which are amplified and conditioned using the charge amplifier. The processed signals are converted to the PC using the data acquisition device. The signals are monitored and processed using DynoWare software. A customized fixture has been used to clamp the workpiece on the dynamometer, which is fixed tightly on the machine tool table.

Design of experiments and data analysis

The experiments have been carried out as a full factorial experiment, where each experiment is replicated three times. The statistical software Minitab has been used to design the experiments and analyze the results. Table 3 shows a sample of 10 experiments out of 144 experiments. For the analysis of this large number of data, analysis of variance (ANOVA) and regression have been performed for each response variable, in addition to using the main trends of them for data visualization.

The strength of the proposed experimental approach is invested in studying three interacting process parameters with three to five levels, unlike the previously published articles in the same topic that

studied only two levels. This approach helps deeply understand and discover advantages and disadvantages of the trochoidal milling process and is needed for optimizing the cutting process. In addition, this experimental methodology will expand and open new applications for the trochoidal milling process. However, other factors such as surface roughness, form accuracy, and tool wear are not included in this research work.

Results and discussion

In this section, the results of experiments regarding cutting forces, material removal rate, and relative specific energy, will be presented and analyzed comprehensively.

Cutting forces

Figure 3 shows an example of the measured cutting forces in x and y directions using the conditions of 6 mm axial depth of cut, 600 mm/min feed rate, and 1 mm trochoidal step. The values of forces vary depending on the tool position in its path and the corresponding chip thickness. The force in x -direction increases to a maximum value, where the cutting force is horizontal and the chip thickness is maximum, where the force in y -direction is almost null. The force in y -direction increases to its maximum value and declines to 0, where the cutting force is horizontal, then it increases in the negative direction, where the cutting forces y -component is in the negative direction. The forces fluctuate due to the intermittent cutting nature of the milling process, while the non-uniformity is due to the presence of tool run-out. The resultant force for the same conditions is shown in Figure 4, the resultant force increases till a maximum value then it decreases to 0. This behavior is similar to that of the chip thickness. It is observed that in the middle area of the curve, the forces do not fall to zero due to the increase of the engagement angle between tool and workpiece, so several teeth are engaged to the workpiece simultaneously.

Effect of axial depth of cut. The maximum resultant force is used to express the cutting forces of each condition. Figure 5 shows the effect of depth of cut on the maximum resultant force at different feed rates and trochoidal step. Generally, for all conditions, the maximum resultant force increases with the axial depth at a rate that depends on the other cutting conditions. As shown in Figure 5(a), for 400 mm/min feed rate and 0.5 mm trochoidal step, the force increases by increasing the axial depth of cut from 2 to 4 mm, then it is kept constant. For the 1 mm trochoidal step, the force is stabilized after 6 mm, while for the 1.5 mm trochoidal step, it is increasing within the full range. This pattern is the same for the other feed rates as

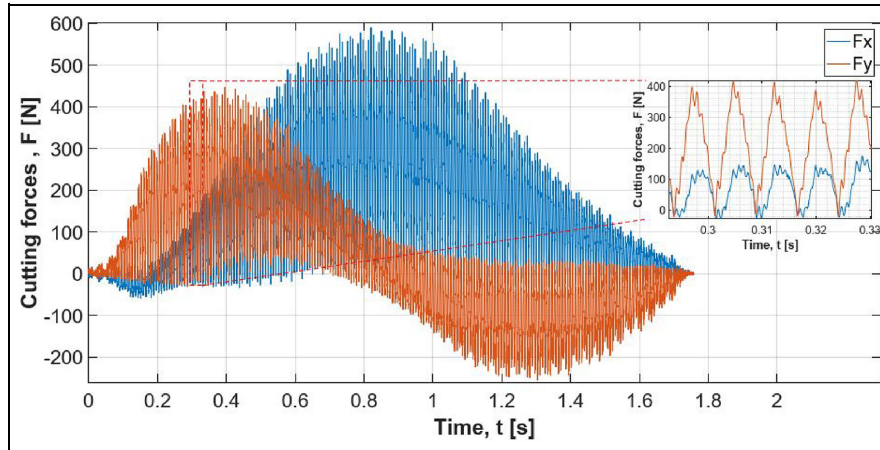


Figure 3. Variation of cutting forces with time for the conditions: 6 mm axial depth of cut, 600 mm/min feed rate, and 1 mm trochoidal step.

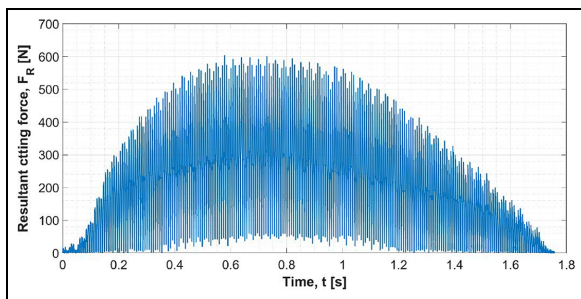


Figure 4. Variation of resultant cutting forces versus time for the conditions: 6 mm axial depth of cut, 600 mm/min feed rate, and 1 mm trochoidal step.

shown in Figure 5(b)–(d). Hence, the threshold of stabilization of the force depends on the trochoidal step and is independent of the feed rate. The threshold of stabilization is 4 and 6 mm for the 0.5 and 1 mm trochoidal step, while for the 8 mm step, this limit is not available for the 1.5 mm trochoidal step. This phenomenon is more clear in Figure 5(e)–(g), for 0.5 and 1 mm trochoidal step and any feed rate, the force is laid out after 4 and 6 mm respectively, while it is always increasing for the 1.5 mm step.

Altıntaş and Lee reported that the maximum engagement angle and the maximum chip thickness are the main parameters affecting cutting forces.³⁵ In order to explain the reason for the discussed trend of the maximum resultant force with the axial depth of cut, the relationship between the axial depth of cut, helix angle, and engagement angle is illustrated in Figure 6. ABCD is the removed chip by the cutting edge and O is the center of the bottom cutting tool circle. The figure shows the maximum engagement angles between the tool and chip at the four depths of cut, using a 1 mm trochoidal step and 600 mm/min. The cutting edge is engaged gradually into the workpiece, increasing the engagement angle between them to a maximum value, where it is kept constant before

disengagement takes place. In the first three cases, Figure 6(a)–(c), the maximum engagement angle is attained when the tool edge intersects the chip at point B. At these positions, the maximum engagement angle is a function of the axial depth of cut, helix angle, and tool radius, equation (2). Hence, by increasing the axial depth of cut or helix angle, or by decreasing the tool diameter, the engagement angle increases significantly, increasing force consequently. Further increase of axial depth of cut, Figure 6(d), the maximum engagement angle is attained when the tool edge intersects the chip at point C. By increasing the axial depth of cut, the engagement will not be increased anymore and so as the cutting forces, as the maximum engagements are the same. The maximum engagement angle, in this case, depends on the trochoidal step, tool radius, and trochoidal radius, equation (3). Therefore, the axial depth of cut does not affect the cutting forces when the cutting edge reaches the exit part of the chip, or in other words when the axial depth of cut is larger than a threshold value $a_{p,th}$. This threshold axial depth of cut depends mainly on tool diameter, tool helix angle, and trochoidal radius, equation (4). For the experiments set, the threshold axial depths of cut are 4.7, 6.7, and 8.4 mm for the trochoidal steps 0.5, 1, and 1.5 mm respectively. These results are consistent with the experimental results presented in the previous section. Figure 7 reveals the effect of axial depth of cut on both maximum engagement angle and maximum resultant force at 600 mm/min feed rate. Both of them stabilize after the same axial depths of cut. For 0.5 and 1 mm trochoidal steps, the maximum engagement angles stabilize after 4.7 and 6.7 mm, accordingly, the forces are kept constant after 4 and 6 mm respectively. For the 1.5 mm trochoidal step, the force is always increasing with the axial depth of cut because the limiting depth is 7.9 mm.

Therefore, in order to limit the increase of engagement angle as the axial depth of cut increases and

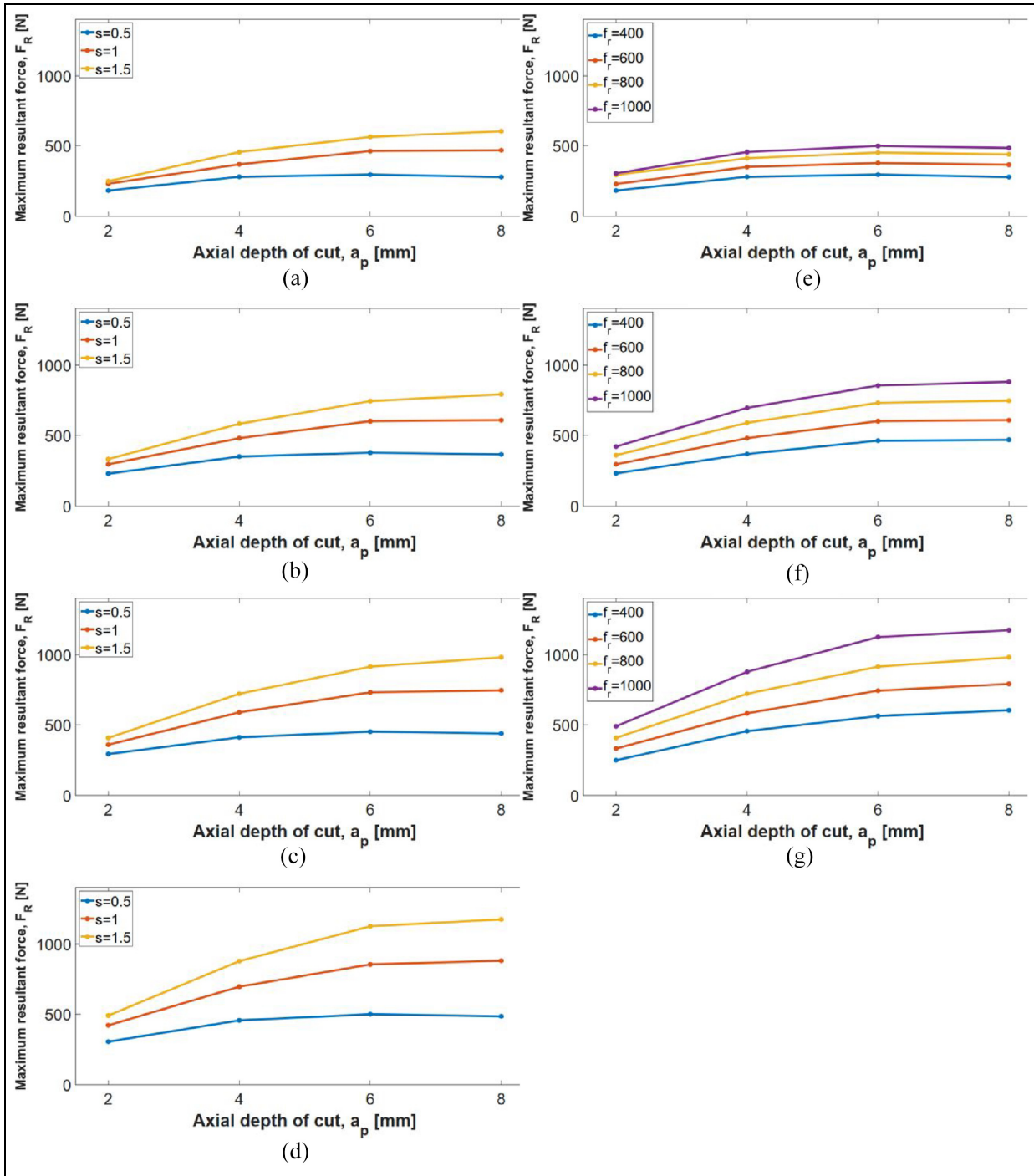


Figure 5. The effect of axial depth of cut on the maximum resultant cutting force at different feed rates and trochoidal steps: (a) $f_r = 400$ mm/min, (b) $f_r = 600$ mm/min, (c) $f_r = 800$ mm/min, (d) $f_r = 1000$ mm/min, (e) $s = 0.5$ mm, (f) $s = 1$ mm, and (g) $s = 1.5$ mm.

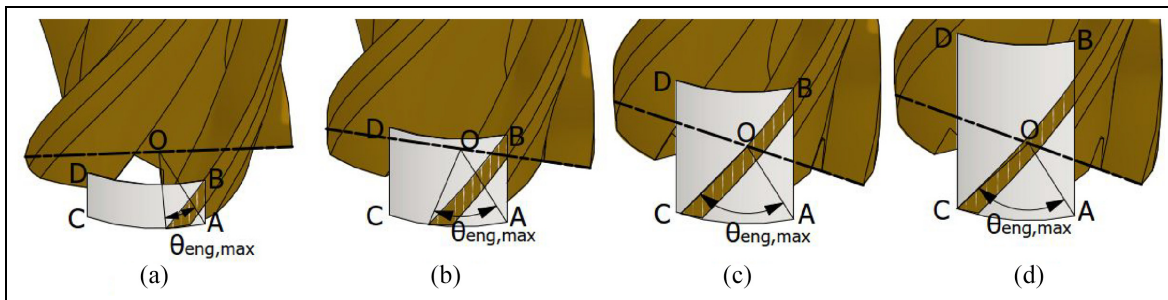


Figure 6. The maximum engagement angle between the tool and workpiece at different axial depths of cut using 1 mm trochoidal step and 600 mm/min feed rate, and (a) 2 mm, (b) 4 mm, (c) 6 mm, and (d) 8 mm axial depths of cut.

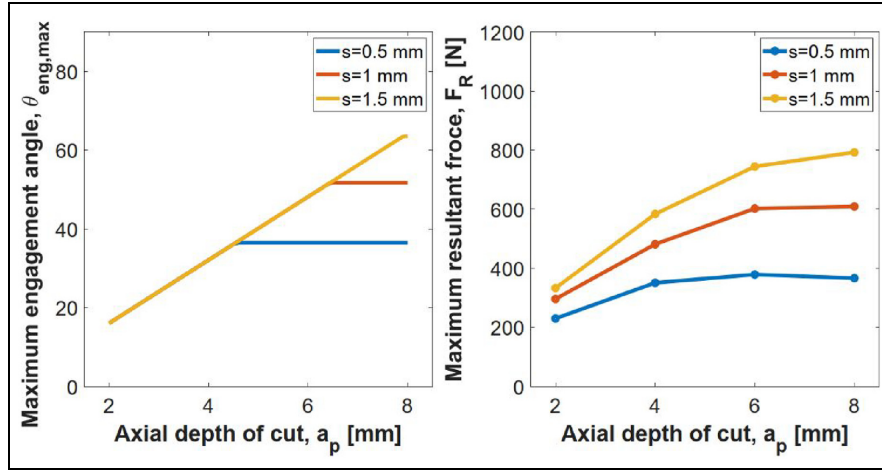


Figure 7. The effect of axial depth of cut on both maximum engagement angle and maximum resultant force at 600 mm/min feed rate and different trochoidal steps.

consequently the cutting force, it is recommended to reduce the threshold axial depth of cut. This can be attained by increasing the helix angle and/or decreasing the tool diameter. It should be considered that increasing the helix angle causes the increase of number of cutting edges in contact, increasing the cutting forces. While tool diameter reduction increases the cycle time, reducing the material removal rate. Hence, optimization of these factors should be implemented.

$$\theta_{eng1} = \frac{a_p \tan(\omega)}{R_t} \quad (2)$$

$$\theta_{eng2} = \pi - \cos^{-1} \left[s \left(\frac{1}{R_{tr}} + \frac{1}{R_t} - \frac{s}{2R_{tr}R_t} \right) - 1 \right] \quad (3)$$

$$a_{p,th} = \frac{R_t}{\tan(\omega)} \left\{ \pi - \cos^{-1} \left[s \left(\frac{1}{R_{tr}} + \frac{1}{R_t} - \frac{s}{2R_{tr}R_t} \right) - 1 \right] \right\} \quad (4)$$

Where (θ_{eng1}), is the maximum engagement angle for the first three cases in Figure 6, (θ_{eng2}) is the maximum engagement angle for the last case in Figure 6, ($a_{p,th}$) is the threshold axial depth of cut, (ω) is the tool helix angle, (R_t) is the tool radius, (R_{tr}) is the trochoidal radius; $R_{tr} = 0.5B - R_t$, and (B) is the slot width.

Effect of feed rate and trochoidal step. The results of the relationship between the feed rate and trochoidal step with the maximum resultant force are shown in Figures 8 and 9. As shown in Figure 8, the maximum resultant force increases with the feed rate by a rate that depends on the other factors. This is due to the increase of the maximum chip thickness, equation (5), and consequently the cutting forces. This rate increases with the increase of trochoidal step as

demonstrated in Figure 8(a)–(d). Figure 8(e)–(g) show the different effects of axial depth of cut on this rate. For the 0.5 mm trochoidal step, the axial depth of cut increase from 2 to 4 mm increases this rate significantly. Whereas for 1 and 1.5 mm trochoidal steps, the ranges of effectiveness of the axial depth of cut are 2–6 and 2–8 mm respectively. This has been explained extensively in the previous section.

Figure 9 demonstrates the relationship between the maximum resultant force and the trochoidal step at different feed rates and axial depths of cut. The maximum resultant force increases significantly with the trochoidal step at a rate that depends on the other factors. This behavior is due to the increase of both the maximum chip thickness and the maximum engagement angle, consequently the cutting forces. This rate increases with the increase of feed rate as demonstrated in Figure 9(a)–(d). Figure 9(e)–(g) shows the different effects of axial depth of cut on this rate, which is similar to that discussed in the relationship between feed rate and maximum resultant force.

$$h_{max} = f_z \sin \left\{ \pi - \cos^{-1} \left[s \left(\frac{1}{R_{tr}} + \frac{1}{R_t} - \frac{s}{2R_{tr}R_t} \right) - 1 \right] \right\} \quad (5)$$

Where (h_{max}) is the maximum chip thickness, and (f_z) is the feed per tooth.

In order to show the contribution of each factor on the maximum resultant force, analysis of variance (ANOVA) of the maximum resultant force has been implemented. Table 4 shows the contribution and significance of each parameter on the maximum resultant force with a 95% confidence level. Since $p < 0.05$ for all the parameters, each has a significant effect on the maximum resultant cutting force. Axial depth of cut and trochoidal step have almost the same influence on the maximum resultant force by 32%, while feed rate has less influence by 7%. Equation (6)

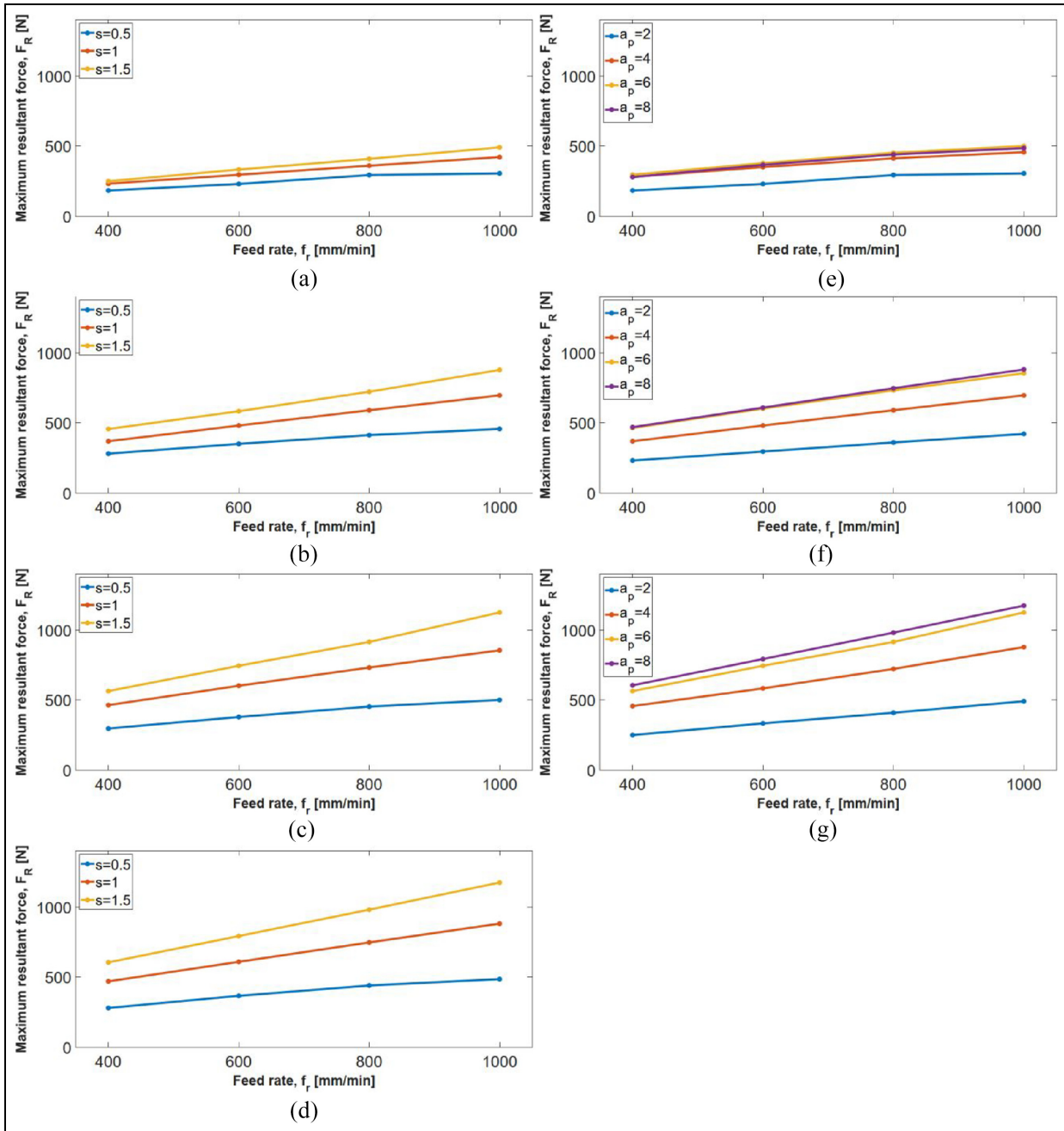


Figure 8. The effect of feed rate on maximum resultant cutting force at different axial depths of cut and trochoidal steps: (a) $a_p = 2$ mm, (b) $a_p = 4$ mm, (c) $a_p = 6$ mm, (d) $a_p = 8$ mm, (e) $s = 0.5$ mm, (f) $s = 1$ mm, and (g) $s = 1.5$ mm.

gives the non-linear regression model of the maximum resultant force as a function of axial depth of cut, feed rate, and trochoidal step with R^2 of 99.7%.

$$\begin{aligned}
 F_{res,max} = & 112.4 - 40a_p - 211.4s + 0.2447f_r + 2.58a_p^2 \\
 & + 73.4s^2 - 0.000318f_r^2 + 112.9a_p s + 0.1031a_p f_r \\
 & - 6.38a_p^2 s - 0.01147a_p^2 f_r - 17.19a_p s^2 + 0.07035a_p s f_r \\
 & - 0.1381s^2 f_r + 0.000264s f_r^2 \quad (6)
 \end{aligned}$$

Material removal rate

In circular-type trochoidal milling the exact material removal rate, MRR , can be calculated from equation (7). Each axial depth of cut, feed rate, and trochoidal step affects the material removal rate significantly. The increase of any of these parameters increases material rate linearly but at different rates, where the increasing rates depend on the other conditions. Figure 10 shows the main trends of MRR concerning

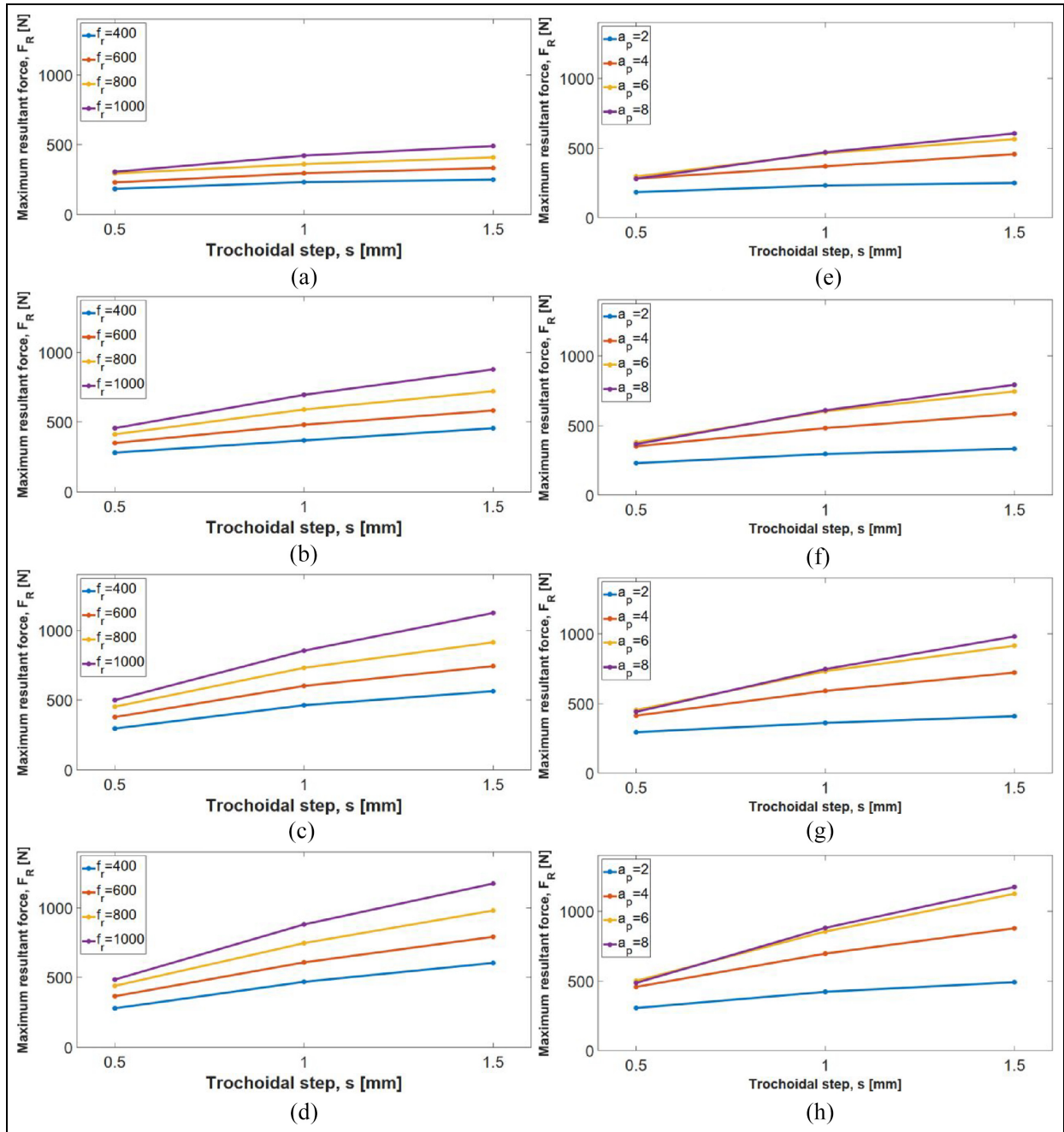


Figure 9. The effect of trochoidal step on maximum resultant cutting force at different axial depths of cut and feed rates: (a) $a_p = 2$ mm, (b) $a_p = 4$ mm, (c) $a_p = 6$ mm, (d) $a_p = 8$ mm, (e) $f_r = 400$ mm/min, (f) $f_r = 600$ mm/min, (g) $f_r = 800$ mm/min, (h) $f_r = 1000$ mm/min,.

Table 4. ANOVA values for the maximum resultant force.

Parameter	SS	DoF	MS	Contribution (%)	F	p
Axial depth of cut, a_p	2,575,249	3	858,416	31	123	< 0.01
Trochoidal step, s	2,665,615	2	1,332,807	32	192	< 0.01
Tool center feed rate, f_r	2,032,730	3	677,577	25	97	< 0.01
Error	939,054	135	6956	11		
Total	8,212,647	143		100		

SS: sum of squares; DoF: degree of freedom; MS: means square; F: F ratio; p: p value.

Table 5. ANOVA values for the material removal rate.

Parameter	SS	DoF	MS	Contribution (%)	F	p
Axial depth of cut, a_p	5,856,392	3	1,952,131	19	18	< 0.01
Trochoidal step, s	9,310,345	2	4,655,172	30	44	< 0.01
Tool center feed rate, f_r	11,478,527	3	3,826,176	37	36	< 0.01
Error	4,173,389	39	107,010	14		
Total	30,818,653	47		100		

SS: sum of squares; DoF: degree of freedom; MS: means square; F: F ratio; p: p value.

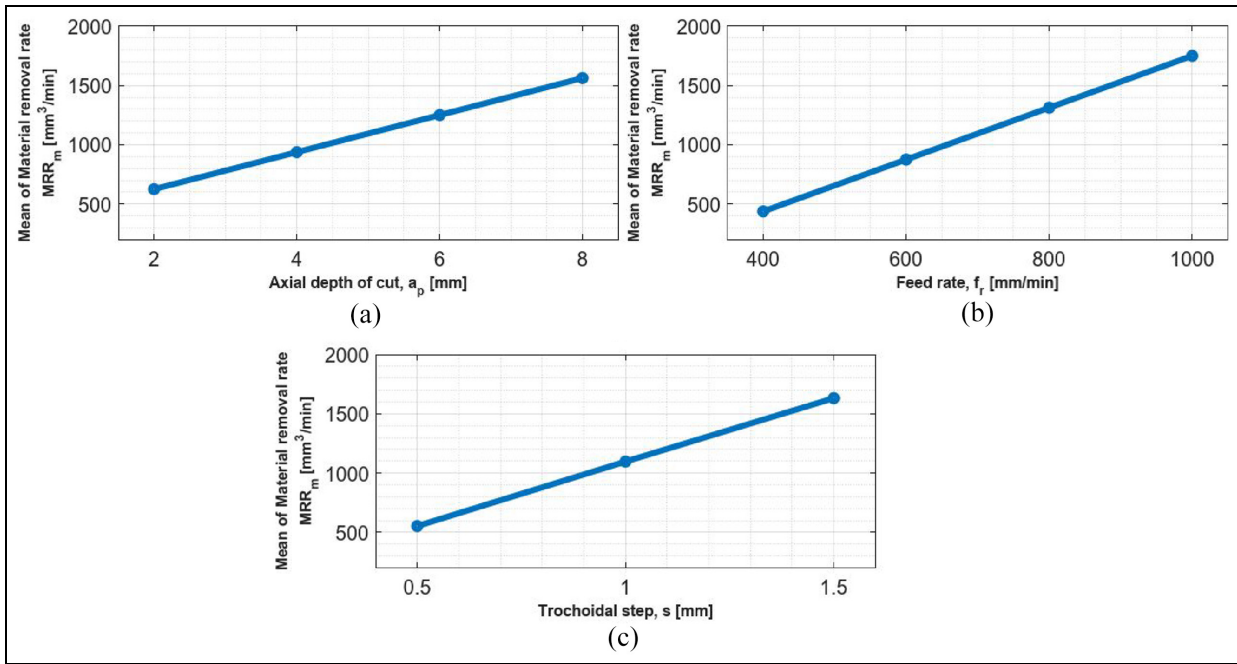


Figure 10. The main trends of the mean of material removal rate as functions of: (a) axial depth of cut, (b) feed rate, and (c) trochoidal step.

the examined parameters. The feed rate has the greatest effect on MRR, followed by the trochoidal step, and finally the axial depth of cut. The ANOVA for MRR presented the contribution of each parameter as in Table 5 for a 95% confidence level. The feed rate of cut has the most contribution on MRR by 37%, followed by the trochoidal step by 30%, and finally the axial depth by only 19%.

$$MRR = \frac{f_r a_p}{s + 2\pi R_T} \left(s R_T + R_T^2 \cos^{-1} C + \frac{1}{2} s R_T C \right) \quad (7)$$

Where (C) is a constant; $C = \sqrt{1 - \left(\frac{s}{2R_T}\right)^2}$.

Relative specific energy

As shown in the previous sections, the increase of either axial depth of cut, feed rate, or trochoidal step, raises both maximum resultant force and material removal rate significantly. The increase in material removal rate is favorable for productivity

enhancement, while the rise of cutting forces increases the consumed energy and reduces both surface quality and accuracy. In order to evaluate the efficiency of trochoidal milling, relative specific energy, U_r , will be utilized. The relative specific energy can be defined as the ratio of the multiplication of maximum resultant force, F_R , and cutting speed, v , to the material removal rate, MRR, equation (8). Figure 11 illustrates the relationship between the machining conditions and the relative specific energy. The cutting conditions have decreasing effects on the relative specific energy because they have larger increasing effects on the material removal rate than on the forces. The axial depth of cut has the largest influence in reducing the relative specific energy, while the trochoidal step has less effect, followed by the feed rate. These results are consistent with the results of Santhakumar and Iqbal, and Oh et al.⁶ These effects are revealed by ANOVA of U_r of 95% confidence level, Table 6. The tool center feed rate has the maximum contribution in decreasing U_r by 57%, followed by the trochoidal step by 24%, while axial depth of cut has the least

Table 6. ANOVA values for relative specific energy.

Parameter	SS	DoF	MS	Contribution (%)	F	p
Axial depth of cut, a_p	1109	3	370	8	10	< 0.01
Trochoidal step, s	3271	2	1636	24	45	< 0.01
Tool center feed rate, f_r	7713	3	2571	57	71	< 0.01
Error	1420	39	36	14		
Total	13,513	47		100		

SS: sum of squares; DoF: degree of freedom; MS: means square; F: F ratio; p: p value.

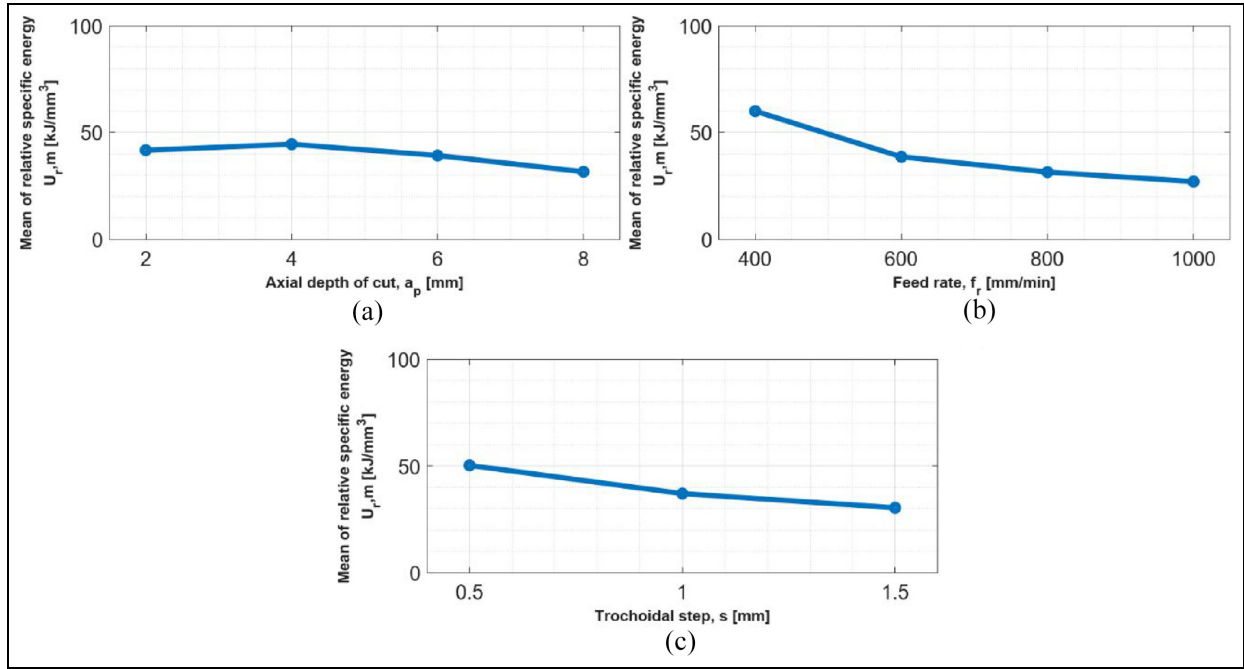


Figure 11. The main trends of the mean of relative specific energy as functions of: (a) axial depth of cut, (b) feed rate, and (c) trochoidal step.

effect by 8%. Therefore, the efficiency of trochoidal milling, in addition to the material removal rate, can be improved by increasing each of the axial depth of cut, trochoidal step, and feed rate. This recommendation is constrained to cutting tool mechanical and thermal properties, machine tool specifications, and surface quality requirements.

$$U_r = \frac{F_{Rv}}{MRR} \quad (8)$$

Conclusions

The findings of this study reveal the major characteristics of trochoidal milling of slots, which are significant for process control and optimization. The effects of cutting conditions: axial depth of cut, feed rate, and trochoidal step, on cutting forces, material removal rate, and specific energy have been experimentally investigated through full factorial design of experiments. The following conclusions were obtained.

- (1). Each of trochoidal step and feed rate shows a linear significant increasing trend with both the maximum resultant force and the material removal rate. The rate of increase depends on the other cutting conditions.
- (2). The increase of axial depth of cut significantly increases the maximum resultant force nonlinearly till a threshold value, where the maximum resultant force does not increase any more. The relationship between the axial depth of cut and material removal rate is linearly increasing. The rate of increase depends on the other cutting conditions.
- (3). The increase of axial depth of cut, feed rate, and/or trochoidal step significantly decreases the specific energy nonlinearly.
- (4). The ANOVA and contribution ratio assessment showed that the trochoidal step and the axial depth of cut have the most influences on the cutting forces by 32% and 31% respectively, while the feed rate has the least contribution by 25%.

- (5). The feed rate has the most contribution in the improvement of material removal rate by 37% followed by the trochoidal step by 30%, and finally the axial depth by 19%.
- (6). The decrease of relative specific energy is induced by the increase of feed rate by 57%, trochoidal step by 24%, and axial depth of cut by 8%.
- (7). In trochoidal milling, it is recommended to machine slots in full depth with high trochoidal step and feed rate, taking into consideration the increase of tool wear and surface roughness. It is preferable to use an endmill with a large helix angle and a small diameter.

However, this study gives a comprehensive investigation of the trochoidal milling, other factors are recommended to be included in the future work, such as surface roughness, form accuracy, and tool wear in a more generalized index.



Declaration of conflicting interests

The author(s) declared no potential conflicts of interest with respect to the research, authorship, and/or publication of this article.

Funding

The author(s) disclosed receipt of the following financial support for the research, authorship, and/or publication of this article: This research work is sponsored by the Egyptian Ministry of Higher Education (MoHE) grant and the Japanese International Cooperation Agency (JICA) in the scope of the Egypt-Japan University of Science and Technology.

ORCID iDs

Mohamed Wagih  <https://orcid.org/0000-0002-3498-1842>
Jiawang Yan  <https://orcid.org/0000-0002-5155-3604>

References

1. Szalóki I, Csuka S, Csesznok S, et al. Can trochoidal milling be ideal. In: *Manufacturing 2012 The XXI. Conference of GTE on manufacturing and related technologies*. Budapest, Hungary, 2012.
2. Salehi M, Blum M, Fath B, et al. Epicycloidal versus trochoidal milling-comparison of cutting force, tool tip vibration, and machining cycle time. *Procedia CIRP* 2016; 46: 230–233.
3. Huang X, Wu S, Liang L, et al. Efficient trochoidal milling based on medial axis transformation and inscribed ellipse. *Int J Adv Manuf Technol* 2020; 111: 1069–1076.
4. Deng Q, Chen ZC, Chang Z, et al. A model for investigating the temperature of trochoidal machining. *J Ind Prod Eng* 2020; 37: 194–203.
5. Liu D, Zhang Y, Luo M, et al. Investigation of tool wear and chip morphology in dry trochoidal milling of titanium alloy Ti-6Al-4V. *Materials* 2019; 12: 1937.
6. Oh NS, Woo WS and Lee CM. A study on the machining characteristics and energy efficiency of Ti-6Al-4V in laser-assisted trochoidal milling. *Int J Precis Eng Manuf Green Technol* 2018; 5: 37–45.
7. Sharif S, Ramli AS, Said AYM, et al. Effect of cutting parameters on tool wear when trochoidal pocket milling Ti6Al4V. *Int J Integr Eng* 2019; 11: 159–165.
8. Deng Q, Mo R, Chen ZC, et al. An analytical approach to cutter edge temperature prediction in milling and its application to trochoidal milling. *Appl Sci* 2020; 10: 1746.
9. Amaro P, Ferreira P and Simões F. Tool wear analysis during duplex stainless steel trochoidal milling. *AIP Conf Proc* 2018; 1960: 070001.
10. Pleta A, Nithyanand G, Niaki FA, et al. Identification of optimal machining parameters in trochoidal milling of Inconel 718 for minimal force and tool wear and investigation of corresponding effects on machining affected zone depth. *J Manuf Process* 2019; 43: 54–62.
11. Ducroux E, Prat D, Viprey F, et al. Analysis and modelling of trochoidal milling in Inconel 718. *Procedia CIRP* 2019; 82: 473–478.
12. Paulo Davim J. *Machining of hard materials*. London: Springer London, 2011.
13. Shixiong W, Wei M, Bin L, et al. Trochoidal machining for the high-speed milling of pockets. *J Mater Process Technol* 2016; 233: 29–43.
14. Deng Q, Mo R, Chen ZC, et al. A new approach to generating trochoidal tool paths for effective corner machining. *Int J Adv Manuf Technol* 2018; 95: 3001–3012.
15. Wang QH, Wang S, Jiang F, et al. Adaptive trochoidal toolpath for complex pockets machining. *Int J Prod Res* 2016; 54: 5976–5989.
16. Uddin MS, Matsubara A, Ibaraki S, et al. Comparison of cutting strategies for high productive end milling. In: *Proceedings of 35th international MATADOR 2007 conference*, 2007, pp.191–194. London: Springer.
17. Waszczuk K, Skowronek H, Karolczak P, et al. Influence of the trochoidal tool path on quality surface of groove walls. *Adv Sci Technol Res J* 2019; 13: 38–42.
18. Szalóki I, Csuka S and Sipos S. New test results in cycloid-forming trochoidal milling. *Acta Polytechnica Hung* 2014; 11: 215–228.
19. Santhakumar J and Iqbal UM. Role of trochoidal machining process parameter and chip morphology studies during end milling of AISI D3 steel. *J Intell Manuf*. Epub ahead of print 2019. DOI: 10.1007/s10845-019-01517-5
20. Amaro P, Ferreira P and Simões F. Comparative analysis of different cutting milling strategies applied in duplex stainless steel. *Procedia Manuf* 2020; 47: 517–524.
21. Santhakumar J and Mohammed Iqbal U. Parametric optimization of trochoidal step on surface roughness and dish angle in end milling of AISID3 steel using precise measurements. *Materials* 2019; 12: 1335.
22. Otkur M and Lazoglu I. Trochoidal milling. *Int J Mach Tools Manuf* 2007; 47: 1324–1332.
23. Hesterberg S and Albert B. Performance and limits of high-dynamic milling processes based on trochoidal tool paths. *Acad J Manuf Eng* 2017; 15: 107–111.
24. García-Hernández C, Garde-Barace J-J, Valdivia-Sánchez J-J, et al. Trochoidal milling path with variable

- feed. Application to the machining of a Ti-6Al-4V Part. *Mathematics* 2021; 9: 2701.
25. Wang Q-H, Liao Z-Y, Zheng Y-X, et al. Removal of critical regions by radius-varying trochoidal milling with constant cutting forces. *Int J Adv Manuf Technol* 2018; 98: 671–685.
 26. David A and Stephenson JSA. *Metal cutting theory and practice*. 3rd ed. Boca Raton: CRC Press, 2016.
 27. Pleta A, Niaki FA and Mears L. Investigation of chip thickness and force modelling of trochoidal milling. *Proc Manuf* 2017; 10: 612–621.
 28. Akhavan Niaki F, Pleta A and Mears L. Trochoidal milling: investigation of a new approach on uncut chip thickness modeling and cutting force simulation in an alternative path planning strategy. *Int J Adv Manuf Technol* 2018; 97: 641–656.
 29. Akhavan Niaki F, Pleta A, Mears L, et al. Trochoidal milling: investigation of dynamic stability and time domain simulation in an alternative path planning strategy. *Int J Adv Manuf Technol* 2019; 102: 1405–1419.
 30. Šajgalík M, Kušnerová M, Harničárová M, et al. Analysis and prediction of the machining force depending on the parameters of trochoidal milling of hardened steel. *Appl Sci* 2020; 10: 1788.
 31. Pleta A, Ulutan D and Mears L. Investigation of trochoidal milling in nickel-based superalloy inconel 738 and comparison with end milling. In: *ASME 2014 International manufacturing science and engineering conference collocated with the JSME 2014 international conference on materials and processing and the 42nd North American manufacturing research conference*, pp. V002T02A058–V002T02A058. Detroit, MI: American Society of Mechanical Engineers.
 32. Waszczuk K. Influence of the trochoidal tool path generation method on the milling process efficiency. *Adv Sci Technol Res J* 2020; 14: 199–203.
 33. Zhao GY, Liu ZY, He Y, et al. Energy consumption in machining: classification, prediction, and reduction strategy. *Energy* 2017; 133: 142–157.
 34. Committee AIH. *ASM handbook, volume 16: machining*. Ohio: ASM International, Electronic, 1989.
 35. Altıntaş Y and Lee P. A general mechanics and dynamics model for helical end mills. *CIRP Ann* 1996; 45: 59–64.